

Commensurability effects in superconducting Nb films with quasiperiodic pinning arrays

M. Kemmler,¹ C. Gürlich,¹ A. Sterck,¹ H. Pöhler,¹ M. Neuhaus,² M. Siegel,² R. Kleiner,¹ and D. Koelle^{1,*}

¹*Physikalisches Institut – Experimentalphysik II, Universität Tübingen,*

Auf der Morgenstelle 14, D-72076 Tübingen, Germany

²*IMS, Universität Karlsruhe, Hertzstr. 16, D-76187 Karlsruhe, Germany*

(Dated: May 25, 2019)

We study experimentally the critical depinning current I_c versus applied magnetic field B in Nb thin films which contain 2D arrays of circular antidots placed on the nodes of quasiperiodic (QP) fivefold Penrose lattices. Close to the transition temperature T_c we observe matching of the vortex lattice with the QP pinning array, confirming essential features in the $I_c(B)$ patterns as predicted by Misko *et al.* [Phys. Rev. Lett **95**(2005)]. We find a significant enhancement in $I_c(B)$ for QP pinning arrays in comparison to I_c in samples with randomly distributed antidots or no antidots.

PACS numbers: 74.25.Qt, 74.25.Sv, 74.78.Na

The formation of Abrikosov vortices in the mixed state of type-II superconductors [1] and their arrangement in various types of "vortex-phases", ranging from the ordered, triangular Abrikosov lattice to disordered phases [2, 3, 4] has a strong impact on the electric properties of superconductors. Both, in terms of device applications and with respect to the fundamental physical properties of so-called "vortex-matter", the interaction of vortices with defects, which act as pinning sites, plays an important role. Recent progress in the fabrication of nanostructures provided the possibility to realize superconducting thin films which contain artificial defects as pinning sites with well-defined size, geometry and spatial arrangement. In particular, artificially produced *periodic arrays* of sub-micron holes (antidots) [5, 6, 7, 8] and magnetic dots [9, 10, 11, 12] as pinning sites have been intensively investigated during the last years, to address the fundamental question how vortex pinning – and thus the critical current density j_c in superconductors – can be drastically increased.

In this context, it has been shown that a very stable vortex configuration, and hence an enhancement of the critical current I_c occurs when the vortex lattice is commensurate with the underlying periodic pinning array. This situation occurs in particular at the so-called first matching field $B_1 = \Phi_0/A$, i.e., when the applied field corresponds to one flux quantum $\Phi_0 = h/2e$ per unit-cell area A of the pinning array. In general, $I_c(B)$ may show a strongly non-monotonic behavior, with local maxima at matching fields $B_m = mB_1$ (m : integer or a rational number), which reflects the periodicity of the array of artificial pinning sites. As pointed out by Misko *et al.* [13], an enhancement of I_c occurs only for an applied field close to matching fields, which makes it desirable to use artificial pinning arrays with many built-in periods, in order to provide either very many peaks in $I_c(B)$ or an extremely

broad peak in $I_c(B)$. Accordingly, Misko *et al.* studied analytically and by numerical simulation vortex pinning by quasiperiodic chains and by 2D pinning arrays, the latter forming a fivefold Penrose lattice [14], and they predicted that a Penrose lattice of pinning sites can provide an enormous enhancement of I_c , even compared to triangular and random pinning arrays. Here, we present results on the experimental investigation of matching effects in superconducting Nb thin films containing various types of antidot configurations. We studied $I_c(B)$ at variable temperature T close to the superconducting transition temperature T_c , and we compare Penrose lattices with triangular lattices, with random arrangements of antidots and with thin films without antidots. Our experimental results on Penrose arrays confirm essential features in the $I_c(B)$ patterns as predicted in [13].

The experiments were carried out on $d = 60$ nm thick Nb films which were deposited by dc magnetron sputtering in the same run on five separate Si substrates covered with a $1\ \mu\text{m}$ thick electrically insulating SiO_2 layer. Patterning was performed by e-beam lithography and lift-off technique to produce cross-shaped Nb bridges with circular antidots arranged in different geometries. Fig. 1(a) shows the geometry of the Nb bridges, allowing four-point measurements in two perpendicular directions on segments of width $w = 200\ \mu\text{m}$ and length (separation between voltage pads) $l = 600\ \mu\text{m}$. On each chip we are able to directly compare eight different cross structures. Six of them contain approximately $N_p = 110,000$ circular antidots with a diameter D of either 250 nm or 400 nm, arranged in either a triangular lattice [Fig. 1(b)], a Penrose lattice [Fig. 1(c)], or in a random arrangement [Fig. 1(d)]. All samples have the same average antidot density $n_p = 0.52\ \mu\text{m}^{-2}$, which corresponds to a first matching field $B_1 = n_p\Phi_0 = 1.08\ \text{mT}$. For reference measurements each chip also contains two cross structures without antidots ("plain" sample).

The fivefold Penrose lattice consists of two types of rhombuses with equal sides $a_P = 1.54\ \mu\text{m}$: "thick" and "thin" ones, with angles $(2\Theta, 3\Theta)$ and $(\Theta, 4\Theta)$, respec-

*Electronic address: koelle@uni-tuebingen.de

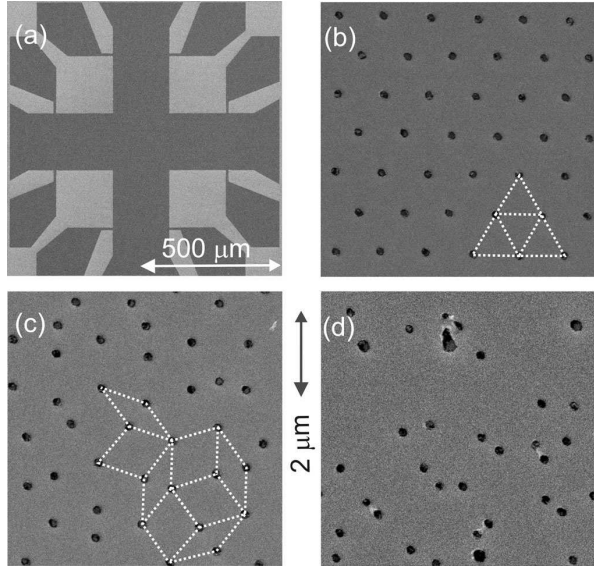


FIG. 1: Scanning electron microscopy images of cross-shaped Nb bridge structure for transport measurements (a), and of different arrangements of antidots (250 nm diameter): triangular lattice (b); Penrose lattice (c); random arrangement (d). The dotted white lines illustrate the lattice geometries.

tively (with $\Theta = 36^\circ$). Accordingly, the small diagonal a_P/τ of the thin rhombuses (i.e., the smallest spacing between two antidots in the Penrose lattice) is $0.952 \mu\text{m}$; $\tau = (1 + \sqrt{5})/2 \approx 1.618$ is the golden mean. The rhombuses have been arranged using inflation rules [14] in order to assure the quasiperiodicity of the antidot lattice. The antidots are placed at the vertices of each rhombus. In Fig. 1(c) some of the antidots are connected by white dashed lines to illustrate the Penrose lattice geometry. In the triangular lattice of antidots the next-neighbor distance is $a_T = 1.49 \mu\text{m}$. For the random arrangement of antidots their x - and y -coordinates were generated by a 2D array filled with uniform random numbers and then scaled to give the same average density of antidots as for the Penrose and triangular lattices.

For electric transport measurements, the samples are mounted in an evacuated chamber which is inserted into a fiberglass cryostat filled with liquid Helium. The cryostat is surrounded by a three-layer magnetic shield and is placed in an rf-shielded room. A superconducting magnet allows to apply a well controlled magnetic field. The sample is mounted together with a Si-diode temperature sensor on a sapphire substrate. Heating the backside of the sapphire substrate (covered by an absorbing layer) via a temperature-stabilized diode laser, the sample temperature can be adjusted from 4.2 K up to 100 K. Using a temperature controller with a PID-feedback loop to control the laser heating power, we achieve a temperature stability, measured at the Si-diode, of about 1 mK. The setup allows to perform electric transport measurements on four bridges on a chip simultaneously.

To characterize our devices, we first measured resis-

tance R vs. T in zero applied magnetic field and determined T_c (with bias current $I = 10 \mu\text{A}$) of the different bridges on each chip. The inset in Fig. 2(a) shows $R(T)$ curves for perforated bridges with antidot diameter $D = 400 \text{ nm}$ and for one bridge without antidots on chip #2. The transition temperature of the perforated bridges ($T_c = 8.660 \text{ K}$) is reduced by 12 mK compared to the bridge without antidots ($T_c = 8.672 \text{ K}$). This can be attributed to a small contamination from the resist structure during Nb film deposition, as we observed a similar behavior on other chips. The perforated bridges also show a larger normal resistance, which can be ascribed to geometry effects and to a slight reduction in the mean free path ℓ_0 as compared to the plain bridges. From the measured resistivity $\rho_{10\text{K}} = 5.52 \mu\Omega\text{cm}$ of the plain film at $T = 10 \text{ K}$ and the relation $\rho\ell_0 = 3.72 \cdot 10^{-6} \mu\Omega\text{cm}^2$ [15] we estimate $\ell_0 \approx 6 \text{ nm}$. We note that we observed for all devices on the same chip always the smallest normal resistance and highest T_c for the plain film, and a similar reduction in T_c for the perforated films. The Penrose and triangular lattices always show a nearly identical resistive transition, whereas the random film usually shows a slightly broadened transition and slightly larger normal resistance. With this respect, the $R(T)$ curves shown in the inset of Fig. 2(a) are representative for all devices on various chips which we investigated. In total we investigated 12 bridges on three different chips (#1, #2, #3). Below we present data for bridges with 400 nm antidots on chips #2 and #3. Bridges with 250 nm antidots on chip #1 behaved similarly.

Figure 3 shows $I_c(B)$ -patterns of a Penrose lattice at three different temperatures close to T_c . For comparison, we insert the calculated $I_c(B)$ dependence (as dashed line), replotted from Fig. 2(e) in [13] (for $N_p=301$ pinning sites), without any adjustable parameter. We find very nice agreement with our experimental data for the two highest temperatures (lower and middle traces): The narrow peak in $I_c(B)$ at $B \approx 0$ broadens above $B/B_1 \approx 0.2$, until a local minimum in $I_c(B)$ is reached at $B/B_1 \approx 0.5$; a two-peak structure appears with I_c maxima at $B/B_1 = 0.81 \approx \tau/2$ (broader peak) and at the first matching field B_1 (narrow peak). Above the first matching field I_c drops rapidly with increasing B . The two-peak structure was predicted in [13] for the case that the gain in pinning energy E_{pin} exceeds the increase in elastic energy E_{el} associated with the deformation of a triangular vortex lattice. Misko *et al.* [13] find the broader peak at a value of $B_{v/t}/B_1 = 0.757$, which corresponds to filling of only three out of four of the pinning sites on the vertices of the thin rhombuses. We find that, with increasing number of inflation steps the number N_p of vertices in our very large Penrose lattices approaches τ (τ^2) times the number of thick (thin) rhombuses (as expected for $N_p \rightarrow \infty$) and $B_{v/t}/B_1$ approaches $\tau/2 \approx 0.809$, which is in excellent agreement with the experimentally observed location of the broader matching peak. In addition, we find at the highest temperature $T/T_c = 0.9988$ a third peak in $I_c(B)$ at $B/B_1 = 0.65 \approx 1/\tau$ [c.f. inset

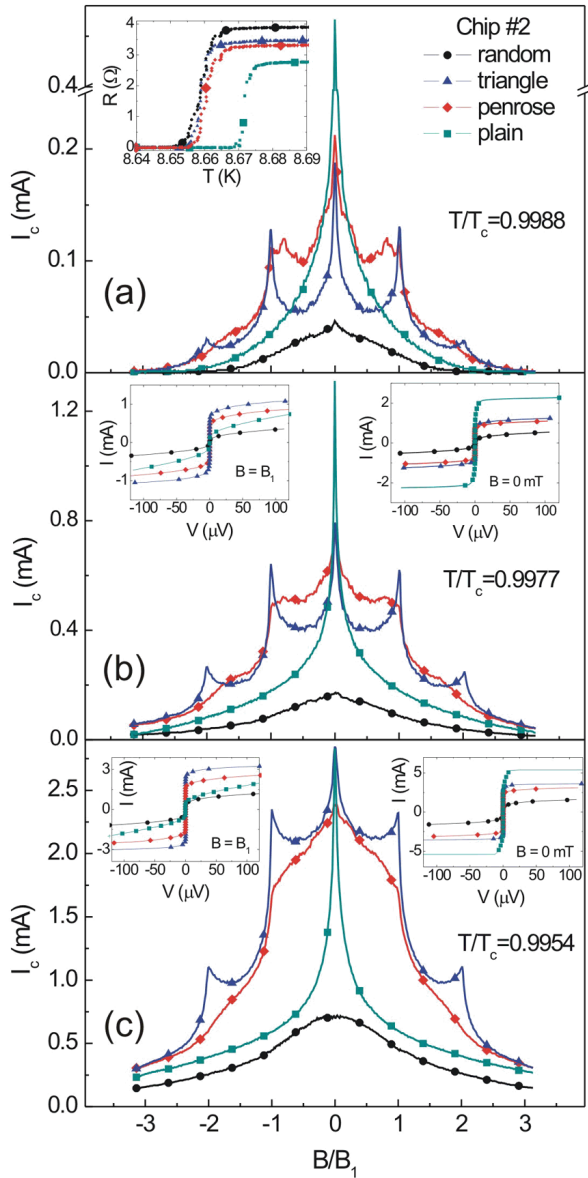


FIG. 2: (Color online) Direct comparison of four different bridges on chip #2, with antidot diameter $D = 400$ nm in the random, triangular and Penrose samples. Main graphs: $I_c(B)$ patterns (voltage criterion $V_c = 2$ μ V); the normalized temperature T/T_c decreases from top (a) to bottom (c). Inset in (a): $R(T)$ curves ($B = 0$; $I = 10$ μ A). Insets in (b),(c): $I(V)$ -curves at $B = 0$ (right) and $B = B_1$ (left).

of Fig. 3]. As the number of thick rhombuses is N_p/τ in the limit $N_p \rightarrow \infty$, this third matching peak can be associated with the occupation of one vortex on one of the vertices on each thick rhombus in our Penrose lattice.

The matching peaks described above are most pronounced at the highest temperature, very close to T_c , and gradually transform into a plateau-like pattern for $I_c(B)$ in the range $0.5 \leq B/B_1 \leq 1$ at the lowest temperature, as shown in Fig. 3. The increase of the (normalized) critical current for $B < B_1$ and the disappearance of the

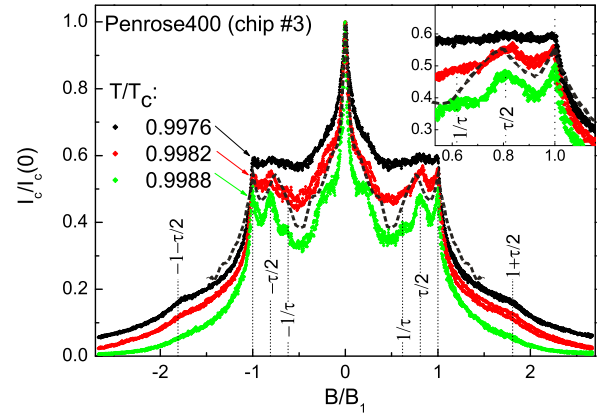


FIG. 3: (Color online) $I_c(B)$ -patterns of a Penrose lattice on chip #3 ($D = 400$ nm) at different temperatures close to $T_c = 8.425$ K ($V_c = 1$ μ V). I_c is normalized to maximum values $I_c(B = 0) = 0.71$ mA, 0.39 mA and 0.16 mA at $T/T_c = 0.9967$, 0.9982 and 0.9988 , respectively. Inset shows magnification at $0.5 \leq B/B_1 \leq 1.15$. For all curves B has been swept through a full cycle (from its minimum value up to its maximum and back). The black dotted lines show the simulation result redrawn from Fig. 2(e) in [13] for $N_p = 301$ pinning sites.

matching peaks with decreasing T can be explained with the decrease of the Pearl length [16] $\Lambda(T) \propto (1 - T/T_c)^{-1}$. For the T -values in Fig. 3 we estimate a change in Λ from ≈ 140 μ m to 40 μ m with decreasing T . Accordingly, the pinning energy increases, leading to an overall increase in I_c and the vortex-vortex interaction range decreases, leading to a smearing and finally vanishing of the matching peaks. The plateau in $I_c(B < B_1)$ is a remarkable feature, which we associate with the effectiveness of the many built-in periods of the Penrose lattice.

With decreasing T another peak-like structure appears at $B/B_1 = 1.77$, close to $1 + (\tau/2)$. In the same T -range, the sample with a triangular lattice and same antidot size (on the same chip) shows with decreasing T the evolution of a clear peak in $I_c(B)$ at the second matching field B_2 . This can be explained by an increase of the saturation number [17] $n_s \approx D/4\xi(T)$ above a value of two (ξ is the coherence length). I.e., by lowering T , pinning of multi-quanta occurs. The observed matching peak at $1 + (\tau/2)$ corresponds then to double occupancy of antidots, except for one antidot on each thin rhombus, which is only occupied by a single vortex. The fact that this matching peak is not very pronounced indicates that E_{pin} only slightly exceeds E_{el} , which also explains the missing of a matching peak at $B = B_2$.

For direct comparison, we simultaneously measured on a single chip (#2) three perforated bridges with different antidot configurations (Penrose, triangular lattice and random; $D = 400$ nm) and one plain bridge. Figure 2 shows their $I_c(B)$ -curves at three different values of T/T_c . In contrast to the plain sample and the sample with random antidot configuration, the Penrose and triangular lattices show clear matching effects, with identical B_1 , as

designed. The triangular lattice shows very pronounced matching peaks at B_1 and B_2 as expected from the absence of the E_{el} -term related to local distortions of a triangular vortex lattice. We do not observe higher order matching peaks, which indicates that $n_s \approx 2$.

The $I_c(B)$ pattern for the Penrose lattice is very similar to the one on chip#3 with same antidot size (c.f. Fig. 3). With decreasing T , the multiple peak structure at $B \leq B_1$ turns into a broad shoulder. When T is lowered further [see Fig. 2(c)], the shoulder transforms into a dome-like structure. We cannot give a concise explanation for the shape of this very broad central peak; however, we note that we observed this on all Penrose lattices which we investigated.

Comparing absolute values of I_c for the Penrose and triangular lattice shows that very close to T_c critical currents at $B = 0$, B_1 and B_2 are quite similar; however, due to the stronger reduction in I_c of the triangular lattice between matching fields, the Penrose lattice is superior, in particular for small fields, below B_1 [see Fig. 2(a)]. This situation changes with decreasing T , as the reduction in I_c of the triangular lattice between matching fields becomes much less pronounced [see Fig. 2(c)]. I. e., we cannot confirm the prediction [13] that the Penrose lattice provides an enormous enhancement in $I_c(B)$ over the triangular one, except for T very close to T_c and fields between $B = 0$ and the first matching field. We should note, however, that even for our devices fabricated within the same deposition run, a direct comparison of absolute values of I_c should be taken with care, as variations in sample quality may have a significant effect, in particular on the T -dependent coherence length and penetration depth close to T_c . This could e.g. explain the significantly larger value of I_c at B_0 for the plain film close to T_c [see Fig. 2(a),(b)]. However, the random antidot arrangement gives always significantly smaller I_c as compared to the other perforated samples with periodic or quasiperiodic antidot arrays, and its I_c is even smaller than I_c of the plain bridge for all fields. This is consistently observed on all chips which we investigated.

Finally, we note that the choice of the voltage criterion V_c for determining I_c does not significantly affect the shape of the $I_c(B)$ -curves discussed above; we checked this for various samples and values of V_c ranging from

10 nV to 10 μ V. For a more detailed analysis, we measured current voltage characteristics (IVCs) of our devices. The insets of Fig. 2(b) and (c) show IVCs of all four bridges at $T/T_c = 0.9977$ and 0.9954, respectively. The IVCs of the perforated bridges evolve smoothly into the resistive state. In particular, there is no sudden change in differential resistance pointing to a sudden increase of the number of moving vortices. At zero field (right hand insets) the IVCs of the different bridges do not cross (this holds up to at least 1 mV). Such a crossing is, however, observed in finite fields. As can be seen in the left hand insets (for $B = B_1$), the differential resistance of the plain bridge is smaller than for the other bridges. Near a voltage of 300 μ V this curve intersects the IVC of the bridges with the triangular and Penrose lattices. A similar crossing is also observed for other values of field and temperatures, however, always well above the threshold voltage V_c used for determining I_c .

In conclusion, we experimentally verified theoretical predictions of the main features of the critical current dependence on the applied magnetic field in a superconducting thin film with a quasiperiodic Penrose lattice of antidots at temperatures close to T_c . In particular, we found matching of the vortex lattice with the quasiperiodic lattice of pinning sites very close to T_c , and we associate various matching peaks in $I_c(B)$ with distinct regular arrangements of the vortices. In addition, we directly compared different arrangements of artificial pinning sites in our Nb films. We find an enhancement of I_c in films with Penrose lattices as compared to films with random arrangement of pinning sites and films without artificial pinning sites, however no significant enhancement of I_c as compared to films with triangular antidot lattices. With respect to applications, it will be interesting to perform more detailed investigations on the effect of optimum antidot size (i.e. saturation number) and density over a wide range of temperatures in quasiperiodic pinning arrays.

We thank Eric Sassier for his support on the measurement setup. This work was supported by the Deutsche Forschungsgemeinschaft (DFG; KL-930/10 and SFB/TR21). M. Kemmler gratefully acknowledges support from the Evangelisches Studienwerk e.V. Villigst.

[1] A. A. Abrikosov, Sov. Phys. JETP **5**, 1174 (1957).
[2] D. R. Nelson and V. M. Vinokur, Phys. Rev. B **48**, 13060 (1993).
[3] G. Blatter *et al.*, Rev. Mod. Phys. **66**, 1125 (1994).
[4] E. H. Brandt, Rep. Prog. Phys. **58**, 1465 (1995).
[5] M. Baert *et al.*, Phys. Rev. Lett. **74**, 3269 (1995).
[6] V. V. Moshchalkov *et al.*, Phys. Rev. B **57**, 3615 (1998).
[7] A. Castellanos *et al.*, Appl. Phys. Lett. **71**, 962 (1997).
[8] K. Harada *et al.*, Science **274**, 1167 (1996).
[9] J. I. Martin, M. Velez, J. Nogues, and I. K. Schuller, Phys. Rev. Lett **79**, 1929 (1997).
[10] D. J. Morgan and J. B. Ketterson, Phys. Rev. Lett. **80**, 3614 (1998).
[11] M. J. Van Bael *et al.*, Phys. Rev. B **59**, 14674 (1999).
[12] J. E. Villegas *et al.*, Phys. Rev. B **68**, 224504 (2003).
[13] V. Misko, S. Savel'ev, and F. Nori, Phys. Rev. Lett. **95**, 177007 (2005).
[14] J.-B. Suck, M. Schreiber, and P. Häussler, eds., *Quasicrystals* (Springer, Berlin, 2002).
[15] A. F. Mayadas, R. B. Laibowitz, and J. J. Cuomo, J. Appl. Phys. **43**, 1287 (1972).
[16] J. Pearl, Appl. Phys. Lett. **5**, 65 (1964).

[17] G. S. Mkrtchyan and V. V. Schmidt, Sov. Phys. JETP **34**, 195 (1972).